Quaternary Geochronology 83 (2024) 101596

Contents lists available at ScienceDirect

Quaternary Geochronology

journal homepage: www.elsevier.com/locate/quageo

Research paper

Luminescence dating of the MIS 6 glaciation of the Pamir mountains (Central Asia)

M.O. Efimova [a,*], E.V. Deev [b], N.A. Taratunina [c], J.-P. Buylaert [c], P.M. Sosin [a], A.V. Panin [a], A.S. Murray [d], R. Schneider [e], M.S. Lukyanycheva [f], O.A. Tokareva [g], O.A. Meshcheryakova [h], R. N. Kurbanov [a]

[a] *Institute of Water Problems, Hydropower and Ecology, NAST, Dushanbe, Tajikistan*
[b] *Institute of Geography, National Academy of Sciences of Kazakhstan, Alma-Aty, Kazakhstan*
[c] *Department of Physics, Technical University of Denmark, Roskilde, Denmark*
[d] *Nordic Laboratory for Luminescence Dating, DTU Physics and Department of Geoscience, Aarhus University, Roskilde, Denmark*
[e] *Uppsala University, Department of Earth Sciences, Uppsala, Sweden*
[f] *Institute of Archaeology, Azerbaijan Academy of Sciences, Baku, Azerbaijan*
[g] *Gorgan University of Agricultural Sciences and Natural Resources, Gorgan, Iran*
[h] *Nanjing University, Nanjing, China*

ARTICLE INFO

Keywords:
Late quaternary
Glaciations
Climate change
Geochronology
Shakhdara range
High Asia
Proglacial lake

ABSTRACT

The Pamir Mountains are one of the highest mountain systems in the world; they act as sources of fresh water for the main rivers of Central Asia: the Amudaria and Syrdaria. Throughout the Quaternary, the Pamirs played a major role in controlling atmospheric circulation and land-surface processes, and provided great volumes of terrigenous sediments for transport by large rivers to the depressions in the Aral and Caspian regions. These ultimately provided broad aeolian cover in the sandy deserts, and finer dust for the widely distributed loess-palaeosol sequences. The glaciation history of this highly dynamic region provides an important basis for understanding climate change, sediment source and landscape evolution in Central Asia during the Quaternary. The question of the number, distribution, extent and timing of Pleistocene glaciations in the Pamir is debated. One of the main obstacles to research, together with difficulties of access and severity of current climate, is the varying degree of preservation of traces of previous glaciations in the western and eastern Pamir. As a result of a geological survey, we for the first time identified a thick lacustrine deposit at high altitudes in a tributary of the Panj – the valley of the Sary-Shitharv River – this records the damming of the Panj River valley by a large glacier. Luminescence measurements were undertaken to obtain the age of the Sary-Shitharv glacially-dammed lake. As often in mountain catchments the quartz OSL signal was unsuitable for dose estimation, and so the chronology of the Sary-Shitharv section is based entirely on post-IR IRSL signals from K-rich feldspar. We used $pIRIR_{50,290}$ and $pIRIR_{200,290}$ protocols and obtained indistinguishable ages from both protocols. Given the high sedimentation rates deduced from the structure of lacustrine deposits, the entire sequence must have been accumulated rather quickly, over a period of no more than a few thousand years. The average age over the whole series of dates is 165 ± 11 ka. This places the existence of the glacially-dammed lake at Sary-Shitharv in late MIS 6, a result that fits well with the general course of the glacial history of the Pamirs.

1. Introduction

The Pamir Mountains in Central Asia are one of the highest mountain systems in the world. Pamir glaciers are sources of fresh water for the main rivers of the region – the Amudaria and Syrdaria. Throughout the Quaternary these large rivers also transported great volumes of sediment, which was then reworked into the Karakum and Kyzylkum deserts. The Pamir Mountains are also located on the border of two atmospheric circulation systems – the Northern Hemisphere westerlies and the monsoon. It has been speculated that strengthening of westerlies and monsoonal circulations in the past could lead to increased precipitation and so glacial advances even in warm periods (Röhringer et al.,

* Corresponding author.
E-mail address: jakovlevamariya@gmail.com (M.O. Efimova).

https://doi.org/10.1016/j.quageo.2024.101596
Received 15 November 2023; Received in revised form 3 July 2024; Accepted 8 July 2024
Available online 14 July 2024

2012); if so, this would decouple glaciations in different parts of the Pamir from global climate trends. Glacial, slope and fluvial sediments from the Pamir are the main source of Quaternary deposits in Central Asia. The Pamir provided material for the large rivers; these filled depressions in the Aral and Caspian regions with sediment, ultimately providing broad aeolian cover in the sandy deserts, and finer dust for the widely distributed loess-palaeosol sequences. Thus, studying the glaciation history of this highly dynamic region provides an important basis for understanding the general patterns of climate change, sediment source, land-surface processes and landscape evolution in Central Asia during the Quaternary.

The question of the number, distribution, extent and timing of Pleistocene glaciations in the Pamir is debated. One of the main obstacles to research, together with difficulties of access and severity of current climate, is the varying degree of preservation of traces of previous glaciations in the Western and Eastern Pamir. In the west, the terrain is sharply dissected vertically, with the relief of up to 5–6 km, giving rise to mainly erosive landscape forms with little preservation of glacial deposits. In the east, in contrast, the mountains form a highland plateau, the valley bottoms are located at ~4 km above sea level, and so the slopes are only weakly dissected. As a result, ancient glaciations in the east can be determined from the almost continuous cover of glacial deposits (Kotlyakov et al., 1993). The first stratigraphic scheme of Pleistocene deposits of Tajikistan was based on the Quaternary glacial complexes of the Western Pamirs (Badakhshan Upper Pleistocene complex, Bartang Middle Pleistocene complex, Kokbai Lower Pleistocene complex) and Eastern Pamirs (Alichur Upper Pleistocene complex, Murgab Middle Pleistocene complex, East Pamir Lower Pleistocene complex) (Vasilyev, 1962). Chedia (1972) divided the glacial history of the broader Pamir-Alay region into three distinct stages. The first occurred during the Early Pleistocene and was characterized by dendrite glaciation covering the river valleys of Western Pamirs and an ice cap in the Eastern Pamirs. Then in the Middle Pleistocene, the glaciers reached their maximum extent for the region. The third glaciation stage in the Late Pleistocene was affected by tectonic uplift in the Western Pamirs; glaciers filled the main western valleys, while in the eastern Pamir glaciers only occupied cirques and kars. By the end of the Late Pleistocene, glaciers began to retreat and left ridges of recessional moraines (Chedia, 1972). Based on geomorphological and stratigraphic analysis, Dodonov (2002) identified four generations of Quaternary moraines in the Eastern Pamirs. In the west, Early and Middle Pleistocene glaciations are only recorded in erosional forms as two complexes of glacial troughs, while for the Late Pleistocene and Holocene at least two generations of moraines can be distinguished (Dodonov, 2002).

In the last 20 years cosmogenic radionuclide dating (CRN) of moraines has allowed researchers to investigate numerical glacial chronologies for various mountain systems in Central Asia: Altay (Gribenski et al., 2016; Blomdin et al., 2018); Tian Shan (Li et al., 2011, 2014; Lifton et al., 2014; Blomdin et al., 2016); Alay (Abramowski et al., 2006; Zech et al., 2013); Western Tibet (Owen et al., 2002, 2006; Hedrick et al., 2011) and others. This has given rise to various palaeoclimatic and palaeoglaciological studies; chronostratigraphic schemes have been proposed, and glacial events in different mountain regions of Central Asia have been correlated (Owen et al., 2012; Stübner et al., 2021). These studies have provided new insights into climate change during the Late Quaternary. A comprehensive study of the Pamir-Alay region (Abramowski et al., 2006) identified eight stages of glacial advance in the Late Quaternary and, for the first time, described the glacial advances at the end of Middle Pleistocene (~136 ka). It was shown that the expansion of glaciation occurred during cold climatic periods, and that the regional Last Glacial Maximum (LGM) occurred earlier than the global LGM due to an increase in climate aridity in the Pamir at the end of the Late Pleistocene. Moreover, glaciers located at high absolute altitudes reached their maximum during MIS 4, whereas those that occupied the lower altitude levels peaked during early MIS 3 due to aridization. The study of the Hissar Range to the west of the Pamirs showed that during the Late Pleistocene glaciers reacted to temperature fluctuations more sharply than those in the Pamir (Zech et al., 2013) and so the regional LGM took place here during MIS 4 and MIS 2, when summer insolation and temperature decreased. This study also assumes the existence of older glaciations that could have developed in the Middle and Early Pleistocene.

Several comprehensive studies of the glacial history of various parts of the Pamir Mountains have been published recently (Abramowski et al., 2006; Zech et al., 2013; Röhringer et al., 2012). Traces of ancient glaciations in the western Pamir have been studied in the valleys of the Shakhdara and Gunt (Stübner et al., 2017) and Bartang (Stübner et al., 2021) rivers. The authors concluded that the most extensive glaciation of the Pamir occurred in the Middle Pleistocene, when a large part of the southeastern Pamirs was probably covered by an ice cap. This ice flowed west, filling the valleys of the main rivers (Shakhdara, Gunt and Panj).

In this paper we contribute to this understanding of the southern Pamir – the region where glacial history of the whole region is best preserved and where the largest Middle Pleistocene glaciations were reconstructed. We present new data on the glacially dammed lake deposits in the tributary valley of Sary-Shitharv; these most probably result from ice filling the Panj River valley. We use luminescence dating to provide a timeframe for this proposed large glaciation of the Southern Pamirs.

2. Study area

The research area lies in the valley of the Sary-Shitharv River, the main right tributary of the Panj River, on the southern slope of the Shakhdara Range (36°52′25.3″N, 72°05′37.5″E) (Fig. 1). Shakhdara Range is in the most southwestern part of the Pamirs, located close to the Tajikistan-Afghanistan border and separated from the Hindu Kush by the deeply incised valley of the Panj river. The range rises to 6726 m. asl. (Karl Marx Peak) and the modern snow line is located at ~5100 m asl. (Zabirov, 1955). The spread of ancient glaciation in the southwestern Pamir was first described by Zabirov (1955) and his map suggests that the entire segment of the Panj river valley parallel to the Shakhdara Range was filled with ice. The southern slope of the Shakhdara Range is characterised by very steep slopes dissected by canyons. Within one of these canyons, 1300 m from the confluence of the Sary-Shitharv River and the Panj River, we identified a unique series of glacial lacustrine deposits (Fig. 2). This series indicates the valley was blocked by a large glacier that filled the valley of Panj River, forming a lake within the Sary-Shitharv tributary. No previous Quaternary geologic studies have been undertaken in the Sary-Shitharv valley.

2.1. Geomorphology

The evolution of the Sary-Shitharv valley is reflected in two sediment sections on the left bank (Fig. 2b). The first sequence is about 2300 m from the confluence of the Sary–Shitharv River with the Panj River within an erosion shadow behind an outcrop of gneiss bedrock. It consists of, at the bottom, alluvium, then glacial sediment with lenses of lacustrine material, and, at the top, deglaciation alluvial deposits. The river has incised ~50 m at this site and the valley base is approximately at an H_{abs} (absolute height) of 2860 m. Bedrock deposits are represented by gneiss. The lower alluvium base is at an H_{abs} of 2869 m, and is represented by ~15 m of boulder pebbles with gray-brown coarse sands interlayers. Sand interlayers have inclined stratification recording the direction of river flow. The moraine deposits are approximately 20 m thick with a base at H_{abs} 2880 m, and are covered by sliding blocks of palaeolacustrine silts up to 1 m thick. These blocks of lacustrine deposits begin to appear within the diamicton at H_{abs} from 2884.5 m up to 2891 m. The deglaciation alluvium lies on top of the moraine deposits and is the highest layer at this site. The alluvium consists of angular granular material within a sandy matrix. The top of the section lies at H_{abs} of 2905 m and corresponds to the highest Sary-Shitharv terrace.

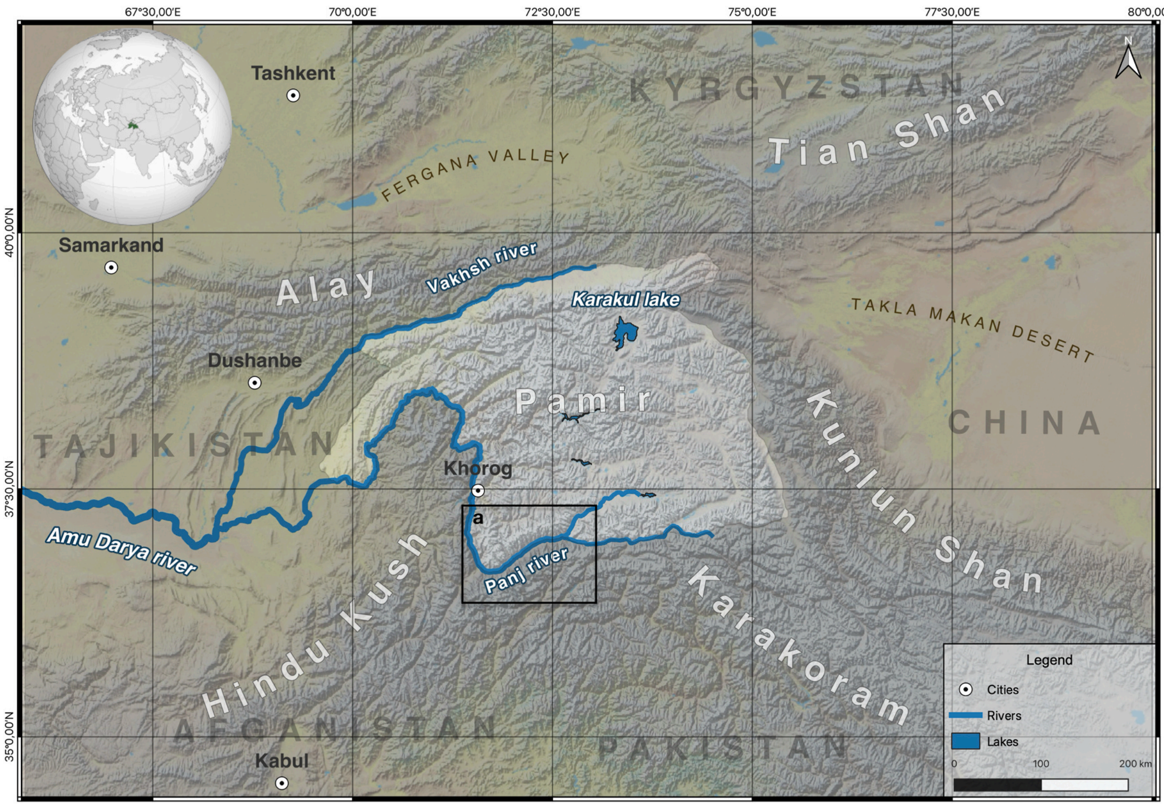

Fig. 1. The Pamir Mountains; a – location of the area investigated in this study in the Southern Pamirs.

The second sequence is about 3300 m from the confluence of the Sary-Shitharv River and the Panj. This 50 m series lies on a diamicton and is covered with alluvium (Fig. 3). The whole sequence forms a terrace at the left side of the valley (Fig. 2A). The lacustrine deposits are visible as separate remnants on the southern and northern slopes of a moraine block partially covered by colluvium. We studied the glaciolacustrine sequence on the northern slope of the moraine block. The glaciolacustrine-moraine contact is ~32 m above the water level of the Sary-Shitharv river (H_{abs} = 2982 m). In the upper part of the section ~82 m above the water level (H_{abs} = 3032 m) there are large erratic granite blocks (~4 m across). Silt layers under these blocks are crushed plastically. These ice-transported blocks probably fell to the bottom of an ancient lake. We interpret the upper deformed layers at the corner of the lacustrine deposits as deformed layers and consider them to be the top of lacustrine series. Deposits of the ancient lake are represented by silts with sandy interlayers, interleaved with layers of well-washed sands. Alluvium with accumulation islands of mobilised boulders (up to ~1 m across) covers the lake sediment sequence.

2.2. Glacially-dammed lacustrine deposits

The section consists of eight units (I-VIII) of glaciolacustrine silt deposits and two thick glaciolacustrine sand layers separating units VI and VII, and VII and VIII (Fig. 3). A major part of the section is composed of thin-layered pale, light beige silts with pale fine sand layers. The silts have a flat platy structure. From the base of the section, silty layers are progressively replaced via medium sand interlayers by coarse-grained material lenses. These lenses are clearly visible at depths of 49.0 m, 45.0 m, 44.5–43.5 m, 42.0–41,5 m, 40.8 m, 38.2 m, 18.0–17.5 m, and 4.0–3.2 m, as folded thick sand layers. Well-sorted massive sands lie between the units in the upper part of the Sary-Shitharv section.

- Unit I is 1.5 m thick. The base of this unit lies at H_{abs} 2982.0 m. It is represented by a parallel subhorizontal layers of fine sands. The middle part of the unit consists of thin-layered pale, light beige silts with pale fine sand interlayers. OSL sample 228427 was taken at 0.5 m. A layer of mudflow deposits with granules and pebbles in sandy matrix forms the upper part of unit I.
- Unit II is 1.2 m thick and includes silts with layers of fine sand. Base of this unit lies at H_{abs} 2983.5 m.
- Unit III is 1.4 m thick and has intensively mixed horizons of fine sands and silts obscuring the pattern of primary sedimentation. The base of this unit lies at H_{abs} 2984.3 m. Samples 228430 and 228431 were taken from the lower and upper parts of this unit.
- A glaciolacustrine sandy layer between Unit III and Unit IV is represented by two layers of medium sand (~0.6 m and ~0.2 m thick) with inclusions of very fine to fine pebbles and two layers (~0.3 m and ~1.1 m thick) of granules and pebbles in sandy matrix.
- Unit IV is 1.1 m thick and consists mostly of interlayered silts and fine sands. The base of this unit lies at H_{abs} 2987.8 m. A layer of medium sand in the lower part of unit lies close to the contact with glaciolacustrine sands. Two samples (228432, 228433) were taken from the Unit's IV lower part.
- In between Unit IV and Unit V is a layer of coarse sand and the layer of pebbles with sandy matrix.
- Unit V has a thickness of 3.44 m and consist of interleaved silts and fine sands. The base of this unit lies at H_{abs} 2990.1 m. Silty layers contain floating surfaces with microbial disturbances. Within these layers there are two layers of rounded granules and pebbles with a sandy matrix in the lower and in the upper parts of the unit. From the lower and the middle parts of Unit V two samples (228435, 228436) were taken.
- Unit VI is 3.44 m thick and represented by silty deposits with fine sand layers. The base of this unit lies at H_{abs} 2993.9 m. Six OSL samples (228437, 228438, 228439, 228440, 228441, 228442) were taken here.
- Well-washed massive sands lie between Unit VI and Unit VII, total thickness ~15.5 m.

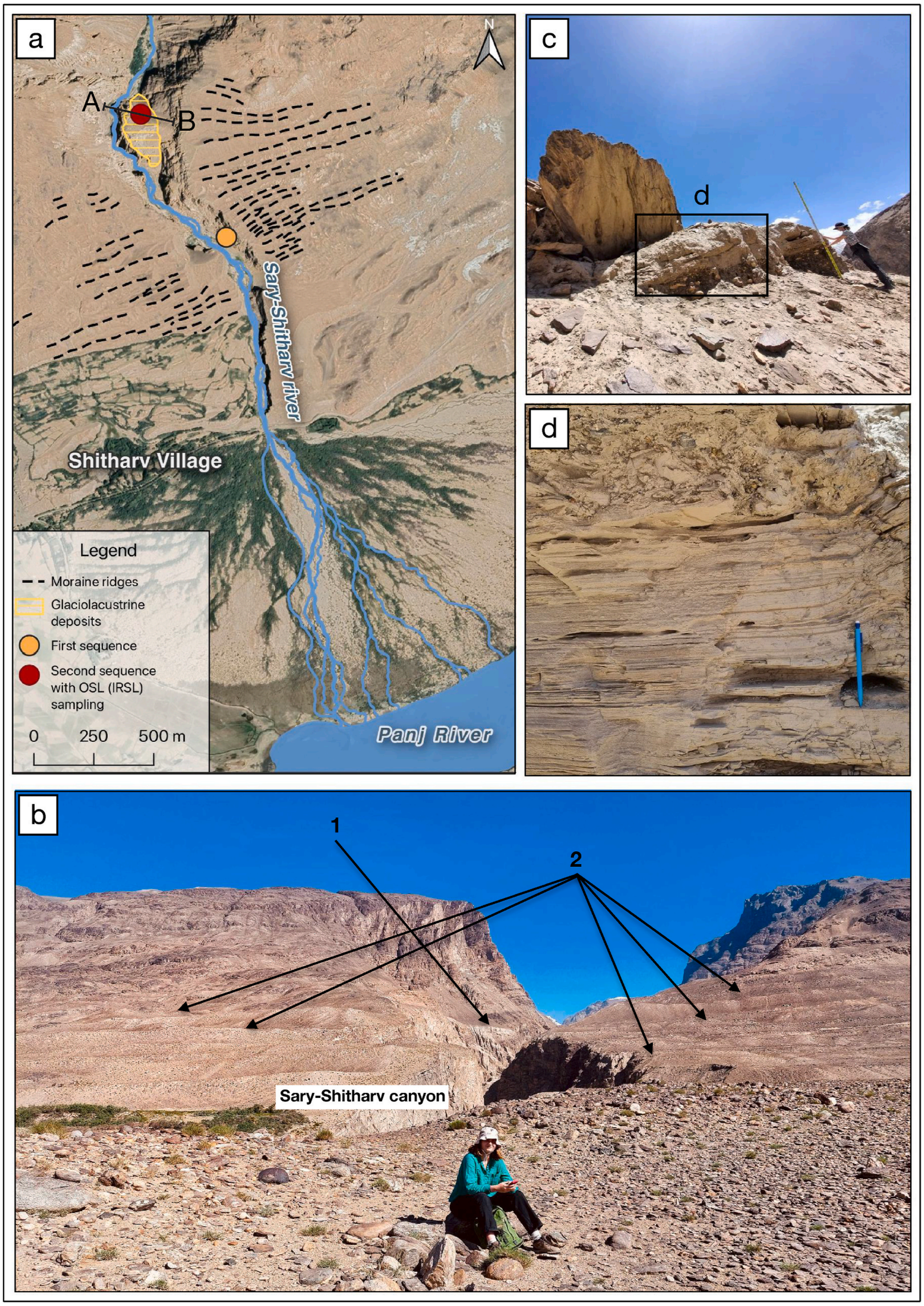

Fig. 2. (a) Physiography of the Sary-Shitharv valley, with the location of the profile A-B (see Fig. 3); (b) general view of the Sary-Shitharv canyon with lacustrine deposits on the right side of the valley (1) and of the southern slope of Shakhdara Range with series of the moraine ridges (2); (c) sections of lacustrine deposits in the northern slope of the moraine block; (d) structure of the lacustrine silts and fine sands.

- Unit VII consists of layers of silts. The base lies at H_{abs} 3012.9 m. In the lower part, there are coarse sandy layers. In the middle of unit there is a layer of rounded granules and pebbles within a sandy matrix. Total thickness of Unit VII is 2.9 m. We took four OSL samples (228443, 228444, 228445, 228446, 228447) from the lower part of the unit with sandy interlayers.

- The interval between Units VII and VIII is represented by sands (8.3 m thick) with a 3.8 m thick layer of silts on the top.

Unit VIII has thickness of 2.1 m. The base of this unit lies at H_{abs} 3027.9 m. There is a 1 m thick layer of coarse gravel in a sandy matrix at the bottom of the unit. Two OSL samples (228449, 228450) were selected from silts above this layer.

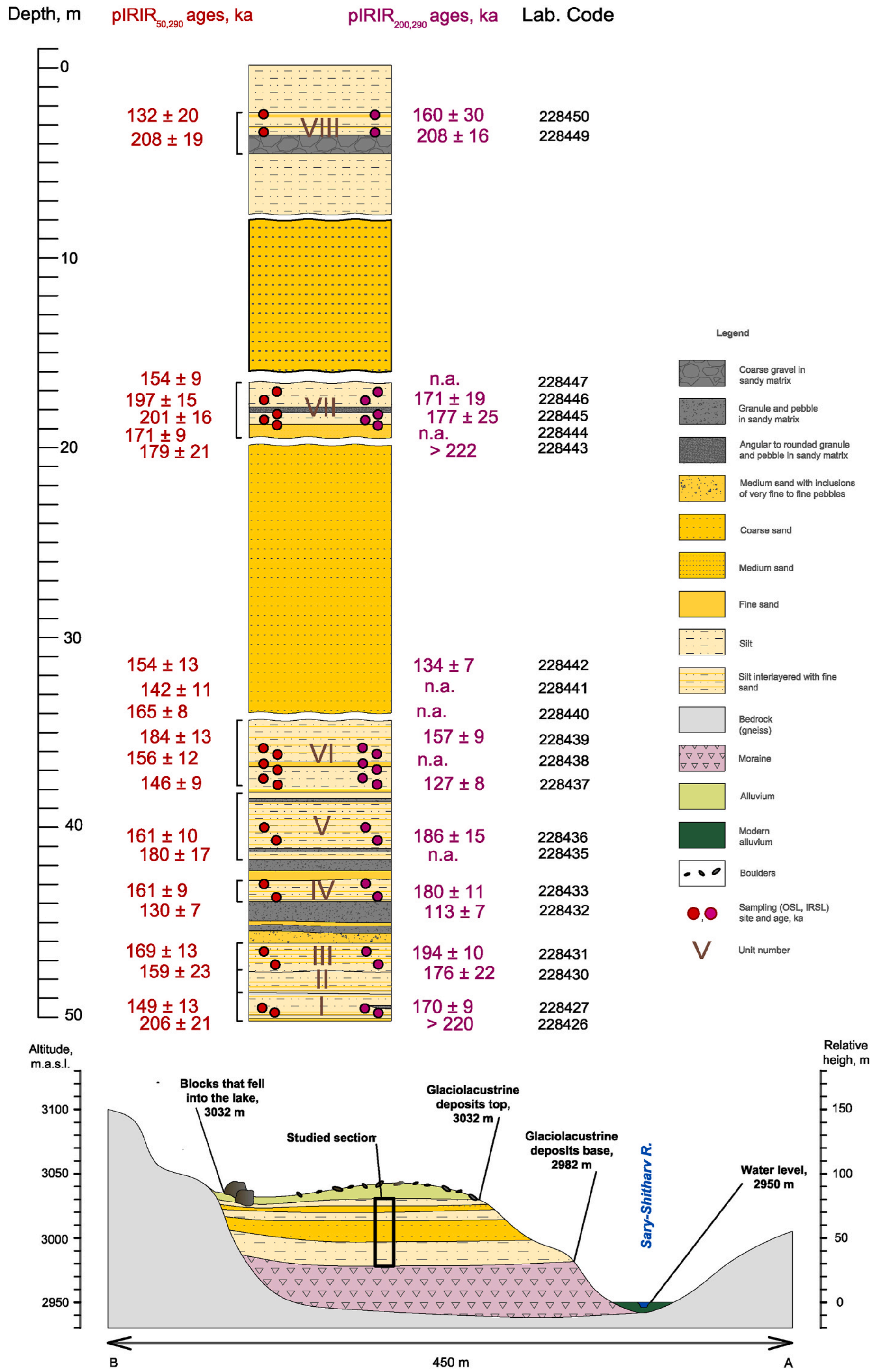

Fig. 3. Sary-Shitharv valley transect with the left bank section. See the location in Fig. 2A.

The uppermost part of the glaciolacustrine deposits is found at the level of 50.5 m above the water level (H_{abs} = 3032.5 m).

3. Sampling and experiments

3.1. Sampling and processing

Fieldwork was carried out in 2022–2023. Within the surface and the northern slope of the inner moraine in the Sary-Shitharv valley seven sections of lacustrine sediments were identified, and 50 m of deposits described. To determine when the lacustrine deposits formed, we took 25 samples for luminescence dating by inserting at least one metallic cylinder into each of the seven sections after cleaning the sediment surface (see Fig. 3, sections are marked with Roman numerals). Potentially bleached material from the ends of the cylinders was removed and used to determine the dose rate (about 150–180 g). Sample preparation included standard chemical procedures (Murray et al., 2021): wet sieving to obtain a fine sand fraction (63–90 μm), followed by treatment with 10% solutions of HCl, H_2O_2, HF, HCl. Chemical cleaning was followed by density separation of quartz/plagioclase and K-rich feldspar using a 2.58 g cm^{-3} sodium polytungstate solution. The heavier quartz/plagioclase fraction was further treated with 40% HF for 1 h for clean the quartz and remove any feldspar and remaining accessory minerals, before a final 10% HCl treatment. From the twenty-five field samples, we obtained K-rich feldspar and quartz grains for twenty-three (two samples were lost during sample preparation).

3.2. Luminescence measurements

Luminescence measurements were undertaken on standard Risø TL/OSL readers equipped with calibrated $^{90}Sr/^{90}Y$ beta sources using Risø calibration quartz mounted on stainless steel cups (Hansen et al., 2018; Autzen et al., 2022). Quartz OSL signals, detected through a Hoya U-340 glass filter, were measured at 125 °C using blue-light stimulation for 40 s using a SAR protocol (Murray and Wintle, 2000, 2003). The quartz OSL signal was dim, with slowly decaying signals and is unsuitable for dose estimation (Wintle and Murray, 2006; Murray et al., 2021); our chronology of the Sary-Shitharv section is based entirely on post-IR IRSL signals from K-rich feldspar.

The equivalent doses of K-rich feldspar fine sand grains (63–90 μm) were determined using SAR post-IR IRSL protocols with first stimulation at 50 °C or 200 °C and subsequent stimulation at 290 °C ($pIRIR_{50,290}$ or $pIRIR_{200,290}$) (Li and Li, 2012; Buylaert et al., 2012). IRSL signals were detected through the blue filter pack (Schott BG3 and BG39 filters). The preheat and cut-heat was 320 °C for 60 s and all IR stimulations lasted for 200s. Late background subtraction was used for net IRSL signal calculation using the initial 2 s minus the last 50 s of the decay curve. No correction was made for possible signal instability. IR_{50}, IR_{200}, $pIRIR_{50,290}$ and $pIRIR_{200,290}$ dose response curves were fitted using *Analyst* v4.57 with a single saturating exponential to derive D_e values (Duller, 2015). A test dose of 30–50% of the measured D_e was used (Yi et al., 2016).

3.3. Dosimetry

Radionuclide concentrations were measured using high resolution gamma spectrometry calibrated using method described in (Murray et al., 1987, 2018). Samples were dried, ground, ignited at 450 °C for 24 h, and mixed with high viscosity wax before casting in a cup-shaped mould. These casts were then stored for 21 days to allow ^{222}Rn to reach equilibrium with its parent ^{226}Ra before analysis. The resulting ^{226}Ra, ^{232}Th and ^{40}K activity concentrations were converted to dry infinite-matrix dose rates following Guérin et al. (2012). Water content corrections were as described by Aitken (1985) and cosmic ray contributions derived from (Prescott and Hutton, 1994). For the calculation of the K-feldspar internal beta dose rate we used the standard assumption of 12.5 ± 0.5% K and a Rb concentration of 400 ± 100 ppm (Huntley and Baril, 1997; Huntley and Hancock, 2001)

4. Results

4.1. Luminescence dating results: dosimetry, luminescence characteristics and ages

Dose rates were calculated from the gamma-spectrometry activity measurements given in Table S1. The radionuclide concentrations are relatively high and do not vary much down the section; total dose rates to feldspar range between 3.25 ± 0.15 and 4.19 ± 0.18 Gy/ka.

The IR_{50}, IR_{200} and $pIRIR_{50,290}$ and $pIRIR_{200,290}$ D_e values are summarized in Tables S2–S3. As expected, the IR_{50} signal gives the lowest D_e values, the IR_{200} D_e values lie in the middle and the $pIRIR_{50,290}$ and $pIRIR_{200,290}$ D_e values are the highest. The IR_{50} to IR_{290} and the IR_{200} to IR_{290} D_e ratios are 0.340 ± 0.011 (n = 19) and 0.79 ± 0.02 (n = 13), respectively. These ratios indicate that both signals are not as stable as the $pIRIR_{290}$ signal and therefore we do not use the IR_{50} and IR_{200} D_e values for age calculation. The average $pIRIR_{50,290}$ to $pIRIR_{200,290}$ D_e ratio is 1.04 ± 0.05 (n = 13) which suggests that an IR_{50} bleach was, for these samples, sufficient to isolate a stable signal (Buylaert et al., 2012). Fig. 4a and b shows a typical feldspar dose response curve for a sample with the natural $pIRIR_{200,290}$ signal in saturation (228426) and one for which it can be easily interpolated on the dose response curve (228432). We have measured in total thirteen $pIRIR_{200,290}$ dose response curves up to 1473 Gy for five samples (228426, 27, 28, 30, 31) and the average $2xD_c$ value from the exponential fit is 773 ± 8 Gy. Based on this value we only give minimum ages for samples with a D_e > 800 Gy.

In terms of laboratory tests, recycling ratios were very close to unity for all signals (e.g. for $pIRIR_{50,290}$: 0.978 ± 0.011, n = 136). We have also carried out a dose recovery test using four samples (228432, 38, 41, 44; 6 aliquots per sample) that were bleached in a solar simulator for 2 days. Three aliquots were used to measure the residual dose and the other set of aliquots was given a large beta doses of 450 or 600 Gy. After subtraction of the residual dose we obtained dose recovery ratios ranging between 1.14 ± 0.07 and 1.39 ± 0.17. Only the lowest ratio can be considered as satisfactory although the larger is only just more than 2σ from unity; this requires further investigation. One possible cause is that bleaching in the solar simulator is causing an unwanted initial sensitivity change for which SAR cannot correct; if so, this is not a problem for measurement of natural signals and doses. Another possibility is an initial sensitivity change during the first heat treatment not successfully corrected for by the natural test dose (e.g. Qin et al., 2018). A SARA measurement (Mejdahl and Bøtter-Jensen, 1994) can test for this, but at the time of writing a suitable young sample to which to add large doses is not available.

There is no trend with depth in the $pIRIR_{50,290}$ ages of Fig. 3 (and

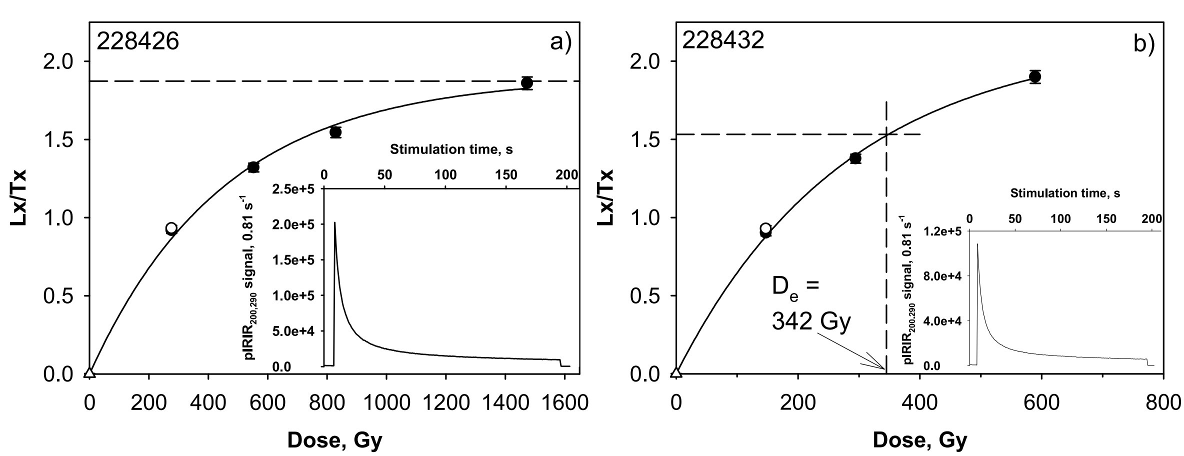

Fig. 4. a) Feldspar $pIRIR_{200,290}$ dose response curve for sample 228426 showing a fully saturated sample (natural level shown as a dashed line). b) Same as in a) but for sample 228432 which is not in field saturation (interpolation of natural signal shown as dashed lines). Recuperation and recycled points are shown as open triangles and open circles, respectively. Insets show natural stimulation curves measured at 290 °C.

Table S2), and the average pIRIR$_{290}$ age (IR$_{290}$ preceded by either IR$_{50}$ or IR$_{200}$) for the entire sequence is 164 ± 4 ka (n = 32, random uncertainties only). Including systematic uncertainty component would give an age of 164 ± 11 ka as the best estimate of the time of sediment deposition. Unfortunately, we do not have a reliable quartz OSL signal in our samples which would allow us to discuss the completeness of bleaching at an individual sample level. However, if we consider the thirty-two finite pIRIR$_{290}$ ages over the 50 m sequence we observe that these data have a relative standard deviation of only 15%. The pIRIR$_{290}$ signals of these samples are not saturated and have clearly been uniformly bleached at some point in the past. If this set of finite ages was affected by partial bleaching, we would expect the standard deviation probably to be considerably larger, since it is difficult to accept that the degree of partial bleaching would remain constant over the thousands of years of deposition represented by this deposit. In our view, the most likely conclusion is that these samples were sufficiently bleached, and that this occurred shortly before or during the last sediment transport.

5. Discussion

5.1. Previous studies of glaciation history of the Pamirs and its mountainous surrounding

The glacial history of the Pamir mountains has been reconstructed earlier using basic geological and geomorphological data, mainly from the correlation with the river terraces (Dodonov, 2002). The first study using numerical dating CRN and ^{14}C was conducted in the southwestern part of the lake Yashilkul basin in the Eastern Pamirs (Zech et al., 2005). They identified four generations of glacier moraines that descended from the Bogchigir Range into the valley of the Alichur and the Gunt rivers. Based on ^{10}Be dating, a first glacial chronology for the Late Pleistocene was obtained: the oldest and most extensive glaciation of the Late Pleistocene took place during the cold phase of MIS 4 (~60 ka), when ice filled the main valley of Yashilkul lake. The next stages of the glacier advance occurred at ~40 and ~27 ka during the cold phases of the MIS 3. The last glaciation occurred at the LGM (~19 ka) and was the smallest in area; this is explained by the increased aridity in Central Asia towards the end of the Late Pleistocene, starving glaciers of precipitation. Further clarification of the glaciation chronology of the Yashilkul lake area showed that local LGM took place during MIS 5, when the valley of the Gunt River and the basin of the lake were filled with ice (Röhringer et al., 2012). The authors explained such scales of glaciation by the intensification of western transport and monsoon circulation. During MIS 2, there were two stages of glacial advance at ~28 ka and 24 ka, and the deglaciation of the area began ~21 ka ago.

A comprehensive study covering the Pamir-Alay region examined traces of glaciation on the Muzkol, Turkestan, Alay, Southern Alichur ranges and in the Yashilkul lake area (Abramowski et al., 2006). This research identified the oldest erratic boulders in the Pamirs, and speculated that they could have been deposited during Early Pleistocene glaciations. However, these yielded ^{10}Be age closer to the Middle Pleistocene (>93–136 ka) and are considered to be underestimates. For the Late Pleistocene, eight stages of glacial advance were determined (~80–60 ka, ~55–40 ka, ~27–25 ka, ~22–20 ka, ~19–17 ka, ~16–15 ka, ~15–13 ka and ~11–9 ka), each becoming smaller in area towards the present. Nevertheless, expansion of glaciation did occur during cold climate periods, despite speculation to the contrary (see Introduction), although the regional LGM occurred earlier than the global LGM due to an increase in climate aridity at the end of the Late Pleistocene. Moreover, glaciers at high absolute altitudes reached their maximum during MIS 4 due to increasing aridity, and those at lower elevations, during early MIS 3.

The study of the Hissar Range glaciation showed that in the Late Pleistocene glaciers in western part of the Pamir-Alay mountain system reacted to temperature fluctuations more sharply than the Pamirs glaciers (Zech et al., 2013). Therefore, regional main glacial advances took place here during MIS 4 and MIS 2, when summer insolation and temperature had decreased. This work also presumed the existence of older Middle and Early Pleistocene glaciations, when the Pamir-Alay territory was at lower altitudes and monsoons could reach the Hissar Range.

In the southeastern Pamirs, studies were conducted in the Tashkurgan valley separating the Pamirs, Karakoram, and Tibet (Owen et al., 2012), and in Waqia Valley, Chinese Pamir (Hedrick et al., 2017). Four moraine complexes were identified in this region: the Dabudaer glacial stage (Middle Pleistocene), the Tashkurgan glacial stage (MIS 4), the Hangdi glacial stage (early MIS 2) and the Kuzigun glacial stage (late MIS 2). In the Waqia valley glacial advances occurred in both early and late MIS 6; these advances probably formed the Waqia Palaeolake during MIS 6, which then drained sometime between ~100 and ~60 ka (MIS 4) (Hedrick et al., 2017). These researchers also noted that local maximum glacial extent was at the beginning of the Late Pleistocene, whereas it occurred during MIS 3 in more southern mountainous areas exposed to the monsoon (Owen et al., 2012).

CRN dating of glacial deposits in the valley of the Muksu River in the Northern Pamirs showed that the only preserved complex of moraines (five lateral and one terminal) in the Fedchenko glacier area was formed during the last glaciation ~17 ka ago during MIS 2 (Grin et al., 2016). The timing of the last glaciation was determined only by one preserved moraine, traces of previous glaciations had been erased either by the last glaciation or by river erosion.

Traces of ancient glaciation in the western Pamir were studied in the valleys of the Shakhdara, Gunt (Stübner et al., 2017, 2024) and Bartang (Stübner et al., 2021) rivers. It was concluded that the most extensive glaciation of the Pamirs occurred in the Middle Pleistocene, when a large part of the Southeastern Pamirs was probably covered by an ice cap. This ice, moving to the west, filled the valleys of the Shakhdara, Gunt and Panj rivers. Our site of Sary-Shitahrv is located in this part of the Panj basin.

5.2. MIS 6 glaciation from luminescence dating

The chronological constraint on the glacial-dammed lake at Sary-Shitharv is based on thirty-two finite pIRIR$_{290}$ ages. The lacustrine-glacial sequence probably represents a single rapid stage of accumulation within a few thousand years or less. Formation of the lake began in late MIS 6, when the glacier that filled the main Panj Valley formed either an ice or moraine dam at the Sary-Shitharv valley outlet. Layers alternating from silts to coarse-grained material within one stratigraphic unit probably reflect changes in the lake regime. Oscillations of a large glacier in the Panj Valley would have affected flow in the glacial dammed lake; lowering the ice level would have drained the lake and led to accumulation of coarse-grained particles. Conversely, ice level increases would have closed the lake, allowing fine particles to accumulate.

The assumption of a large glacier in the Panj River valley during the most widespread glaciation was first proposed by Zabirov (1955). According to the altitude of the palaeo-equilibrium line altitude (ELA - elevation where annual accumulation and ablation are equal, a direct proxy for annual mass balance), Zabirov suggested that the dendritic glacier was located along the southern foot of the Shakhdara Range in the upper reaches of the Panj River. It formed at the confluence of glaciers descending mainly from the lateral gorges of the Hindu Kush and partly from the Shakhdara and Ishkashim ranges near from highest peaks – Karl Marx (6723 m), Engels (6507 m) and Mayakovskiy (6096 m). The Pamir and Wakhandarya rivers valleys, which at the confluence form the Panj river, were ice-free.

Thick glacial deposits have been described before in the upstream Panj and in the Pamir River and Wakhandaria River valleys (Stübner et al., 2017). These moraines were formed by a large valley glacier which existed during the most extensive documented glaciation in the southern Pamir. This dendrite glacier extended westward from the south east Pamir Plateau; the latter was covered by an ice cap in the Middle Pleistocene. The timing of this glacier was assumed from the CRN ages of two roches moutonnées (142 ± 10 ka, recalculated in Stübner et al., 2021) located close to the lateral moraine ridge in the lower Gunt Valley, 200 km downstream. At this site, the moraine material is ~200–300 m thick and roches moutonnées are ~110 m above the valley floor. The boulder ages (188 ± 15 ka) of the 50–100 m thick diamictic hummocky deposits of the Bachhor unit (Stübner et al., 2024), located in the higher Gunt Valley, provide further evidence for the glaciation time.

Absolute dating of the Middle Pleistocene deposits in the Pamirs is rare. In the overwhelming majority of the Central Asian regions, the glacial chronology covers only the last glacial cycle (Zech et al., 2005; Seong et al., 2009; Owen et al., 2012) with the oldest dated glacial advance in Pamir placed within MIS 5 (Rhöringer, 2012). Our new data fit well with the modern glacial chronology for MIS 6 in the Pamirs. Glaciers of the arid regions of Central Asia, to which the Pamirs belong, peaked between MIS 6 and MIS 4; during MIS 2–3, glaciation cover was much smaller (Batbaatar, 2018). Boulders of a Middle Pleistocene moraine (the matrix of which has been completely washed away) were described in the Kol-Uchkol–Gurumdy area (SE Pamir). The moraine has been left by an MIS 6 or even earlier glacial advance (Abramowski et al., 2006). In Gissar Valley, to the west of the Pamir, the most extensive glaciation(s) occurred during MIS 6 or earlier and had an ELA depression of ~550 m (2300 m–3400 m) (Zech et al., 2013). As for the SW Pamirs, based on the results of studies in the lower reaches of the Gunt River, it was concluded that the most extensive glaciation of the Pamirs could have been either a single stage or several stages during the Middle Pleistocene (MIS 8, 10 or 12), up to MIS 6 (Karasu, Dabudaer stages) (Stübner et al., 2021, 2024).

Our new dating results obtained for the Sary-Shitharv are also in good agreement with data from the Waqia valley (Chinese Pamir), where a large Waqia Palaeolake may have been glacially dammed (Hedrick et al., 2017). The lacustrine deposits in this lake are also composed of thick beds of laminated silts with thin lenses of granules and pebbles clasts. The glacial advance in the Waqia valley began in the early MIS 6 or earlier and took place up to the late MIS 6. During MIS 6 the Waqia Paleolake had a stage of lacustrine and fluvial deposition (~208-103 ka).

6. Conclusion

The glacial history of the Pamir mountains has been reconstructed earlier mainly using geological and geomorphological data, and, in recent years, CRN dating. In the southeastern Pamirs, a region where the glacial history of the whole region is best preserved, traces of the most extensive glaciation were identified for the Middle Pleistocene, when a large part of the mountains was probably covered by an ice cap which, when moving to the west, filled the large river valleys Shakhdara, Gunt and Panj (Stübner et al., 2021, 2024). As a result of geomorphological studies and geological surveys we for the first time identified a thick lacustrine deposit at high altitudes in the main tributary of the Panj – the valley of the Sary-Shitharv River. These lacustrine series indicate that the valley was blocked by a large glacier filling Panj River valley, and formed a lake within the Sary-Shitharv tributary. We used two signals from K-rich feldspars $pIRIR_{50,290}$ and $pIRIR_{200,290}$ to obtaining luminescence age control. The ages from both protocols are indistinguishable, and do not change systemjatically over the 50 m sediment sequence; these ages place the glacially-dammed lake at Sary-Shitharv valley in MIS 6 (average age: 165 ± 11 ka, n = 32). The pIRIR age is in good agreement with the existing CRN chronology on roches moutonnées (142 ± 10 ka) at the lower reaches of Gunt river, a valley ~200 km downstream from Sary-Shitharv. Our pIRIR ages are also in good agreement with data from the Waqia valley (Chinese Pamir), where a large Waqia Palaeolake may have been glacially dammed by glacial advance in the early MIS 6 (Hedrick et al., 2017). Thus, we conclude that The MIS 6 age of the Sary-Shitharv glacially-dammed lake fits into the framework of the glacial history of the Pamirs.

CRediT authorship contribution statement

M.O. Efimova: Writing – review & editing, Writing – original draft, Visualization, Investigation, Conceptualization. **E.V. Deev:** Investigation, Data curation. **N.A. Taratunina:** Visualization, Methodology, Investigation. **J.-P. Buylaert:** Writing – review & editing, Writing – original draft, Supervision, Methodology, Investigation, Conceptualization. **P.M. Sosin:** Resources, Investigation, Data curation. **A.V. Panin:** Writing – review & editing, Supervision, Project administration. **A.S. Murray:** Writing – review & editing, Supervision, Methodology, Formal analysis. **R. Schneider:** Investigation. **M.S. Lukyanycheva:** Investigation. **O.A. Tokareva:** Investigation. **O.A. Meshcheryakova:** Investigation. **R.N. Kurbanov:** Writing – review & editing, Supervision, Project administration, Data curation, Conceptualization.

Declaration of competing interest

The authors declare that they have no known competing financial interests or personal relationships that could have appeared to influence the work reported in this paper.

Data availability

Data will be made available on request.

Acknowledgments

This work was partly supported by NordForsk through the funding to "The timing and ecology of the human occupation of Central Asia", project number 105204.

Appendix A. Supplementary data

Supplementary data to this article can be found online at https://doi.org/10.1016/j.quageo.2024.101596.

References

Abramowski, U., Bergau, A., Seebac, D., Zech, R., Glaser, B., Sosin, P., Kubik, P.W., Zech, W., 2006. Pleistocene glaciations of Central Asia: results from ^{10}Be surface exposure ages of erratic boulders from the Pamir (Tajikistan), and the Alay–Turkestan range (Kyrgyzstan). Quat. Sci. Rev. 25, 1080–1096. https://doi.org/10.1016/j.quascirev.2005.10.003.

Aitken, M.J., 1985. Thermoluminescence Dating. Academic Press, London.

Autzen, M., Andersen, C.E., Bailey, M., Murray, A.S., 2022. Calibration quartz: an update on dose calculations for luminescence dating. Radiat. Meas. 157, 106828. https://doi.org/10.1016/j.radmeas.2022.106828.

Batbaatar, J., 2018. Quaternary Glaciation in Central Asia (Doctoral Dissertation).

Blomdin, R., Stroeven, A.P., Harbor, J.M., Lifton, N.A., Heyman, J., Gribenski, N., Petrakov, D.A., Caffee, M.W., Ivanov, M.N., Hättestrand, C., Rogozhina, I., 2016. Evaluating the timing of former glacier expansions in the Tian Shan: a key step towards robust spatial correlations. Quat. Sci. Rev. 153, 78–96. https://doi.org/10.1016/j.quascirev.2016.07.029.

Blomdin, R., Stroeven, A.P., Harbor, J.M., Gribenski, N., Caffee, M.W., Heyman, J., Rogozhina, I., Ivanov, M.N., Petrakov, D., Walther, M., Rudoy, A.N., Zhang, W., Orkhonselenge, A., Hättestrand, C., Lifton, N.A., Jansson, K.N., 2018. Timing and dynamics of glaciation in the Ikh Turgen mountains, Altai region, high Asia. Quat. Geochronol. 47, 54–71. https://doi.org/10.1016/j.quageo.2018.05.008.

Buylaert, J.P., Jain, M., Murray, A.S., Thomsen, K.J., Thiel, C., Sohbati, R., 2012. A robust feldspar luminescence dating method for Middle and Late Pleistocene sediments. Boreas 41, 435–451. https://doi.org/10.1111/j.1502-3885.2012.00248.x.

Chedia, O.K., 1972. South of Central Asia in the Modern Era of Mountain Formation. Ilim, Frunze (In Russ.).

Dodonov, A.E., 2002. The Quaternary of Middle Asia (Doctoral Dissertation) (in Russ.).

Duller, G.A.T., 2015. The Analyst software package for luminescence data: Overview and recent improvements. Ancient TL 33, 35–42.

Gribenski, N., Jansson, K.N., Lukas, S., Stroeven, A.P., Harbor, J.M., Robin, B., Ivanov, M. N., Jakob, H., Petrakov, D.A., Alexei, R., Tom, C., Lifton, N.A., Caffee, M.W., 2016. Complex patterns of glacier advances during the late glacial in the Chagan Uzun Valley, Russian Altai. Quat. Sci. Rev. 149, 288–305. https://doi.org/10.1016/j.quascirev.2016.07.032.

Grin, E., Ehlers, T.A., Schaller, M., Sulaymonova, V., Ratschbacher, L., Gloaguen, R., 2016. ^{10}Be surface-exposure age dating of the Last Glacial Maximum in the northern

Pamir (Tajikistan). Quat. Geochronol. 34, 47–57. https://doi.org/10.1016/j.quageo.2016.03.007.

Guérin, G., Mercier, N., Nathan, R., Adamiec, G., Lefrais, Y., 2012. On the use of the infinite matrix assumption and associated concepts: a critical review. Radiat. Meas. 47, 778–785. https://doi.org/10.1016/j.radmeas.2012.04.004.

Hansen, V., Murray, A., Thompsen, K., Jain, M., Autzen, M., Buylaert, J.−P., 2018. Towards the origins of over-dispersion in beta source calibration. Radiat. Meas. 157−162. https://doi.org/10.1016/j.radmeas.2018.05.014.

Hedrick, K.A., Seong, Y.B., Owen, L.A., Caffee, M.C., Dietsch, C., 2011. Towards defining the transition in style and timing of Quaternary glaciation between the monsoon-influenced Greater Himalaya and the semi-arid Transhimalaya of Northern India. Quat. Int. 236, 21–33. https://doi.org/10.1016/j.quaint.2010.07.023.

Hedrick, K.A., Owen, L.A., Chen, J., Robinson, A., Yuan, Z., Yang, X., Imrecke, D.B., Li, W., Caffee, M.W., Schoenbohm, L.M., Zhang, B., 2017. Quaternary history and landscape evolution of a high-altitude intermountain basin at the western end of the Himalayan-Tibetan orogen, Waqia Valley, Chinese Pamir. Geomorphol 284, 156–174. https://doi.org/10.1016/j.geomorph.2016.09.002.

Huntley, D.J., Baril, M.R., 1997. The K content of the K-feldspars being measured in optical dating or in thermoluminescence dating. Anc. TL 15, 11–13.

Huntley, D.J., Hancock, R.G.V., 2001. The Rb contents of K-feldspar grains being measured in optical dating. Anc. TL 19, 43–46.

Kotlyakov, V.M., Rototaeva, O.B., Lebedeva, I.M., 1993. Glaciation of the Pamir–Alai mountains. Nauka, Moscow (in Russian).

Li, B., Li, S.H., 2012. A reply to the comments by Thomsen et al. on "Luminescence dating of K-feldspar from sediments: a protocol without anomalous fading correction.". Quat. Geochronol. 8, 49–51. https://doi.org/10.1016/j.quageo.2011.10.001.

Li, Y.K., Liu, G.N., Chen, Y.X., Li, Y.N., Harbor, J., Stroeven, A.P., Caffee, M., Zhang, M., Li, C.C., Cui, Z.J., 2014. Timing and extent of Quaternary glaciations in the Tianger Range, eastern Tian Shan, China, investigated using ^{10}Be surface exposure dating. Quat. Sci. Rev. 98, 7–23. https://doi.org/10.1016/j.quascirev.2014.05.009.

Li, Y.K., Liu, G.N., Kong, P., Harbor, J., Chen, Y.X., Caffee, M., 2011. Cosmogenic nuclide constraints on glacial chronology in the source area of the Urumqi River, Tian Shan, China. J. Quat. Sci. 26, 297–304. https://doi.org/10.1002/jqs.1454.

Lifton, N., Beel, C., Hättestrand, C., Kassab, C., Rogozhina, I., Heermance, R., Oskin, M., Burbank, D., Blomdin, R., Gribenski, N., Caffee, M., Goehring, B.M., Heyman, J., Ivanov, M., Li, Y.N., Li, Y.K., Petrakov, D., Usubaliev, R., Codilean, A.T., Chen, Y.X., Harbor, J., Stroeven, A.P., 2014. Constraints on the late Quaternary glacial history of the Inylchek and Sary-Dzaz valleys from in situ cosmogenic ^{10}Be and ^{26}Al, eastern Kyrgyz Tian Shan. Quat. Sci. Rev. 101, 77–90. https://doi.org/10.1016/j.quascirev.2014.06.032.

Mejdahl, V., Bøtter-Jensen, L., 1994. Luminescence dating of archaeological materials using a new technique based on single aliquot measurements. Quat. Geochronol. (QSR) 13, 551–554.

Murray, A.S., Arnold, L.J., Buylaert, J.-P., Guérin, G., Qin, J., Singhvi, A.K., Smedley, R., Thomsen, K.J., 2021. Optically stimulated luminescence dating using quartz. Nat. Rev. Methods Primers 1, 72. https://doi.org/10.1038/s43586-021-00068-5.

Murray, A.S., Helsted, L.M., Autzen, M., Jain, M., Buylaert, J.P., 2018. Measurement of natural radioactivity: calibration and performance of a high-resolution gamma spectrometry facility. Radiat. Meas. 120, 215–220. https://doi.org/10.1016/j.radmeas.2018.04.006.

Murray, A.S., Marten, R., Johnston, A., Martin, P., 1987. Analysis for naturally occurring radionuclides at environmental concentrations by gamma spectrometry. J. Radioanal. Nucl. Chem. 115, 263–288. https://doi.org/10.1007/BF02037443.

Murray, A.S., Wintle, A.G., 2000. Luminescence dating of quartz using an improved single-aliquot regenerative-dose protocol. Radiat. Meas. 32, 57−73..

Murray, A.S., Wintle, A.G., 2003. The single aliquot regenerative dose protocol: potential for improvements in reliability. Radiat. Meas. 37, 377−381.

Owen, L.A., Chen, J., Hedrick, K.A., Caffee, M.W., Robinson, A.C., Schoenbohm, L.M., Yuan, Z., Li, W., Imrecke, D.B., Liu, J., 2012. Quaternary glaciation of the Tashkurgan valley, Southeast Pamir. Quat. Sci. Rev. 47, 56–72. https://doi.org/10.1016/j.quascirev.2012.04.027.

Owen, L.A., Finkel, R.C., Ma, H., Barnard, P.L., 2006. Late Quaternary landscape evolution in the Kunlun Mountains and Qaidam Basin, Northern Tibet: a framework for examining the links between glaciation, lake level changes and alluvial fan formation. Quat. Int. 154/155, 73–86. https://doi.org/10.1016/j.quaint.2006.02.008.

Owen, L.A., Kamp, U., Spencer, J.Q., Haserodt, K., 2002. Timing and style of Late Quaternary glaciation in the eastern Hindu Kush, Chitral, northern Pakistan: a review and revision of the glacial chronology based on new optically stimulated luminescence dating. Quat. Int. 97–98, 41–55. https://doi.org/10.1016/S1040-6182(02)00050-2.

Prescott, J.R., Hutton, J.T., 1994. Cosmic ray contributions to dose rates for luminescence and ESR dating: large depths and long-term time variations. Radiat. Meas. 23, 497–500. https://doi.org/10.1016/1350-4487(94)90086-8.

Qin, J., Chen, J., Li, Y., Zhou, L., 2018. Initial sensitivity change of K-feldspar pIRIR signals due to uncompensated decrease in electron trapping probability: evidence from radiofluorescence measurements. Radiat. Meas. 120, 131–136. https://doi.org/10.1016/j.radmeas.2018.06.017.

Röhringer, I., Zech, R., Abramowski, U., Sosin, P., Aldahan, A., Kubik, P.W., Zöller, L., Zech, W., 2012. The late Pleistocene glaciation in the Bogchigir Valleys (Pamir, Tajikistan) based on ^{10}Be surface exposure dating. Quat. Res. 78 (3), 590–597. https://doi.org/10.1016/j.yqres.2012.09.002.

Seong, Y.B., Owen, L.A., Yi, C., Finkel, R.C., 2009. Quaternary glaciation of Muztag Ata and Kongur Shan: evidence for glacier response to rapid climate changes throughout the late glacial and holocene in westernmost Tibet. Geol. Soc. Am. Bull. 121 (3–4), 348–365. https://doi.org/10.1130/B26339.1.

Stübner, K., Grin, E., Hidy, A.J., Schaller, M., Gold, R.D., Ratschbacher, L., Ehlers, T., 2017. Middle and Late Pleistocene glaciations in the southwestern Pamir and their effects on topography. Earth Planet Sci. Lett. 466, 181–194. https://doi.org/10.1016/j.epsl.2017.03.012.

Stübner, K., Bookhagen, B., Merchel, S., Lachner, J., Gadoev, M., 2021. Unravelling the Pleistocene glacial history of the Pamir mountains, Central Asia. Quat. Sci. Rev. 257, 1–15. https://doi.org/10.1016/j.quascirev.2021.106857.

Stübner, K., Gadoev, M., Rugel, G., Lachner, J., Bookhagen, B., 2024. Three Pleistocene glacial advances and a warm episode during MIS-3: towards a more complete glacial history of the Pamir mountains. Quat. Sci. Adv. 13, 100135 https://doi.org/10.1016/j.qsa.2023.100135.

Vasilyev, V.A., 1962. Stratigraphy of Quaternary deposits of Tajikistan. The newest stage of geol. development of the territory of Tajikistan. Dushanbe: Tajik Academy of Science, SSR (In Russian).

Wintle, A.G., Murray, A.S., 2006. A review of quartz optically stimulated luminescence characteristics and their relevance in single-aliquot regeneration dating protocols. Radiat. Meas. 41, 369–391.

Yi, S., Buylaert, J.−P., Murray, A.S., Lu, H., Thiel, C., Zeng, L., 2016. A detailed post−IR IRSL dating study of the Niuyangzigou loess site in northeastern China. Boreas 45, 644–657. https://doi.org/10.1111/bor.12185.

Zabirov, R.D., 1955. Oledenenie Pamira. GeografGIZ, Moskva (in Russian).

Zech, R., Abramowski, U., Glaser, B., Sosin, P., Kubik, P.W., Zech, W., 2005. Late Quaternary glacial and climate history of the Pamir Mountains derived from cosmogenic ^{10}Be exposure ages. Quat. Res. 64 (2), 212–220. https://doi.org/10.1016/j.yqres.2005.06.002.

Zech, R., Rhöringer, I., Sosin, P., Kabgov, H., Merchel, S., Akhmadaliev, S., Zech, W., 2013. Late Pleistocene glaciations in the Gissar Range, Tajikistan, based on ^{10}Be surface exposure dating. Palaeogeogr. Palaeoclimatol. Palaeoecol. 369, 253–261. https://doi.org/10.1016/j.palaeo.2012.10.031.